ISSN: 2320-1983 Print ISSN: 2320-1991 Online Volume 1 Issue 1

Applied Cell Biology

Regular Paper

ACB, 1(1), 2012 [4-15]

Nucleotide radicals in DNA/RNA synthesis. Computational approach

Alexander A.Tulub[1,2]

[1]University of Manchester, Oxford Road, Manchester, M13 9PL, (UK)

[2]Saint-Petersburg State University, Universitetskaya Emb. 7/9, 199034, Saint-Petersburg, (RUSSIAN FEDERATION)

Received: 3rd September, 2012 ; Accepted: 20th November, 2012

ABSTRACT

A new radical mechanism of nucleotide polymerization is found. The finding is based on the Car-Parrinello molecular dynamics computations at 310 K with an additional spin-spin coupling term for ^{31}P and ^{1}H atoms and a radical pair spin term included. The mechanism is initiated by a creation of a high-energy spin-separated Mg-ATP complex in a triplet state in which the Mg prefers an uncommon chelation to the O2-O3 oxygens of the ATP. The cleavage of the complex produces the ! AMP^- and ! O^- radicals. The latter captures a proton from acidic solution (the Zundel cation) that converts it into the ! OH radical. The process agrees with the proton-coupled electron transfer (PCET) mechanism. Through interacting with the HO-$C_{3'}$ group of the deoxyribose/ribose the ! OH radical captures its hydrogen atom. The process is accompanied by producing water and the ! AMP radical. The ! AMP^- and AMP radicals then interact yielding a dimer. The described mechanism is easily generalized for a bigger number of adjoining nucleotides and their type. The radical mechanism is highly sensitive to the ! AMP^-" ! OH radical pair spin symmetry and the radius of the ! OH diffusion. This confines the operation of the radical mechanism: it is applicable to nucleotide polymerization through the HO-$C_{3'}$ group of deoxyribose/ribose (DNA/RNA polymerization) and inapplicable through the HO-$C_{2'}$ group of ribose (RNA) " a result that nature has developed over evolution. # 2012 Trade Science Inc. - INDIA

INTRODUCTION

Little historical background seems appropriate to preface the paper.

When Isaac Newton published his *Principia Mathematica*[1], 1687, which supreme achievement was the construction of a universal theory of gravity and inertia, he was severely blamed for his discoveries by many of the then outstanding mathematicians and philosophers, including Gottfried von Leibniz, René Descartes, and Samuel Clarke. Although Newton was able to mathematically describe gravity's action on bodies, he created a philosophical controversy by being unable to describe the mechanism by which it acted. The lack of clarity in mechanisms of gravity action created around Newton's gravity theory the aura of mystery until the nature of gravitation was revealed in the 20th century.

The same aura of mystery surrounds the nature of genetic code and gene expression. Everyone today implicitly accepts James Watson and Francis Crick's theory[2] postulating that DNA is the storage of genetic information. Numerous experiments confirm the validity of their theory: protein synthesis is a result of a step-by-step transfer of information encoded in DNA fragments through RNA(s) operating as peculiar information messengers. These are observable and undisputed facts. But like with the gravity theory of Newton's time we practically know nothing about the physical principles underlying the process of information transfer – what sort of information reads RNA on DNA matrix and how then this information affects creating unique

amino acids. Hydrogen bonding, no doubt, provides recognition between DNA strands and DNA-RNA short fragments. But the bonding is no more than a stabilization factor of electrostatic nature between the partners. Any attempts to reveal an encrypted code in two or three hydrogen bonds between the complementary DNA/RNA nucleotides fell short[3].

We are not that naïve as to assert that next pages will give answers to the origin of the genetic code – no way! The problem will be narrowed to giving a new insight into DNA/RNA nucleotide polymerization based on spin conversions. Our deep belief is that spin activation/suppression is a driving force leading us to understanding the nature of the genetic code hidden in the triplet nucleotide sequences of DNA strands.

COMMON AND RECENT VIEWS ON NUCLEOSIDETRIPHOSPHATE CLEAVAGE

In a living cell a polynucleotide synthesis proceeds along a chain of DNA nucleotides (template) with a special holoenzyme - DNA polymerase[4,5]. The enzyme's action is closely related to the activity of associated with its structure Mg^{2+} cations whose role in the polynucleotide synthesis is still unclear[6-10]. It is proved that the adjoining of a new nucleotide to the growing polynucleotide chain occurs through the cleavage of a corresponding NTP (N = A, G, C, Thy (U in RNA)) to NMP[5,6]. The cleavage is commonly assumed to be a purely hydrolytic (ionic) process yielding the NMP in a $\{BR(P_\alpha O_4)H_2\}$ (B-base, R-deoxyribose/ribose) form with the phosphorus atom P_α bound to four oxygen atoms[6]. The diester bond formation between the adjoining nucleotide and the polynucleotide chain (polymerization) is also viewed as a hydrolytic process yielding as a side product a water molecule arising through interaction between the negatively charged OH^- group of NMP and the proton H^+ of the ribose hydroxyl. We have outlined this, widely accepted mechanism of the diester bond formation[4-7], to stress its purely ionic nature that initially excludes any spin effect: the initial, intermediate and final products are in the same S state. Everything seems fine, but why the presence of Mg (without it no cleavage or synthesis occurs[8-10]) is that essential? The question has no answer and serves the topic of vigorous disputes[11,12]. If the role of Mg is reduced only to polarization of P-O bonds that favors the NTP hydrolysis (the common view), then Mg could be easily replaced by other cations, say Ca^{2+}, Be^{2+}, Zn^{2+}, $Mn^{2+/4+}$ or $Fe^{2+/3+}$, because the triphosphate core of NTP is flexible enough to adjust to chelation with each of the said cations showing the similar polarization effect on the P-O bonds[4,7,11]. The unique nature of Mg is traced not only in polynucleotide chain synthesis but in many other NTP-involved reactions like PCR[13], tubulin assembly into MTs[12], myosine dynamics[15,16], and intra-, inter-cellular signaling[5,17].

Our previous works show why Mg and not other cation is required in NTP cleavage[18,19]. The history of the finding goes back to explanation of the mechanism of the Grignard reaction (Victor Grignard, the Nobel prize in Chemistry, 1912) in the metal organic chemistry. Any attempts to initially use Zn instead of Mg fell short in Grignard's experiments[20]. The advantage of Mg over Zn and other cations is that Mg is capable easily to change its oxidation number from zero (metal) to +2 including an intermediate state with the oxidation number +1[21]. This intermediate state corresponds to arising a spin separated complex of T state: $\bullet Mg^+$ and $\bullet R{-}X$ (R = C_2H_5, CH_3 etc, X = halogen). The state is unstable and makes the R-X bond become longer that allows the Mg atom to get inserted between the R and X. At the final stage we see the formation of the R-Mg-X complex (the Grignard reagent) in S state. The Grignard reaction comes from a CI between the T and S PESs. In case of Mg the CI is easily reached while in case of Zn the T and S states do not cross revealing a remarkable gap between them (for details see[21]).

A similar picture appears with the Mg^{2+} cation when it binds NTP in cellular media. A spin symmetry of the Mg-NTP complex can be easily changed from S to T upon a slight excitation. This, particularly, is observed in case of the $Mg^{2+}(Asp)_2$ complex embedded into the DNA-polymerase hydrophobic/hydrophilic pocket, Figure 1. The pocket possesses two sites, B and A, exposed to Mg^{2+} cation binding[9]. The B-site is catalytic, which function is to activate the A-site. Normally, the Mg(B) atom bonds Asp256, Asp190, O_α of the triphosphate tail of NTP, Figure 3 (left part), O_3 of the primer and a water molecule (in Figure 1 N = C). In this environment the Mg(B) reveals the oxidation number +1 (S state). The Mg^{2+}(A) normally bonds Asp192, a water molecule and O_β - O_γ oxygens of the NTP. The activation of the A-site occurs upon bonding the rest

Regular Paper

unbound oxygen of Asp190. When the bonding occurs, S and T PESs intersect creating a CI point[22]. The produced NTP-Mg(B)-Asp190-Mg(A)-NTP chain favors immediate charge redistribution (Figure 2): NTP^{4-} donates its electron to Mg^{+}(B), which becomes uncharged and loses its bond with O_{α}. At the same time the excess of charge on the Mg(B) transfers through Asp190 onto the Mg(A), which gains the charge +1. The Mg^{+}(A)-NTP^{-3} is a biradical complex, in which unpaired spins (T state) are located on the Mg and NTP fragments, respectively.

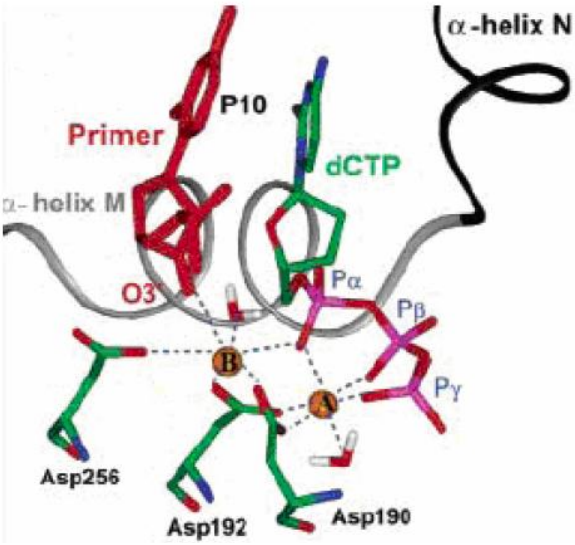

Figure 1 : Hydrophobic/hydrophilic magnesium pocket of the poly-DNA/dCTP complex (reproduced from kind permission of the authors of[9]). Two Mg^{2+} sites are labeled as B (catalytic) and A (nucleotide-binding). The details see in text.

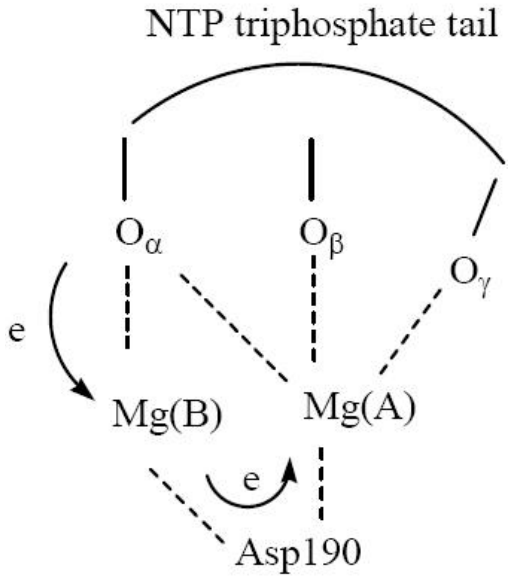

Figure 2 : Schematic picture of electron transfer in a chain NTP-Mg(B)-Asp190-Mg(A)-NTP upon chelation of Asp190 (details see in text and Figure 1).

As it was proved before, the Mg^{+}-NTP^{-3} (hereinafter we omit the notation A to one of the Mg sites) undergoes a rapid decomposition according to reaction (1)[19,22]

$$[(H_2O)_2Mg^{+}\bullet\text{-}\bullet NTP^{-3}]^{SS} \xrightarrow{\text{unstable}} 2PO_3^{-} + Mg^{+}(H_2O)_2 + O + \bullet NMP^{-} \quad (1)$$

Here instead of Asp is used H_2O that simplifies MD calculations. Reaction (1) produces the radical $\bullet NMP^{-}$ and atomic oxygen O, which initiate ion-radical polymerization of DNA (or RNA in case of RNA polymerase) strand (see below). The production of $\bullet NMP^{-}$ was confirmed by CIDNP on ^{31}P nuclei which showed stable polarization effect in the interval $10^{-12} \div 10^{-7}$ s[23].

A strong contrast between the radical and ionic cleavage is that the first mechanism yields a highly active radical – $\bullet NMP^{-}$ – while the second gives a purely inert ionic form – NMP^{2-}. In addition, the structure of $\bullet NMP^{-}$ and NMP^{2-} shows a remarkable difference – in the $\bullet NMP^{-}$ the phosphorus atom P_{α} is bound to three oxygen atoms while in the NMP^{2-} (hereinafter NMP) it is bound to four oxygens. Reaction (1) assumes its further progress involving the attack of its radical products, see below, their potential cellular targets – the inert NMPs or their strings – polynucleotide chains.

AIMS AND SCOPE

The paper aims to prove that

i) the AMP polymerization (without loss of generality, in our computational experiment NTP/NMP ≡ ATP/AMP) has the radical nature: it originates from the cleavage of the unstable $[\bullet Mg^{+}(H_2O)_2\text{-}\bullet A\grave{O}P^{3-}]^{SS}$ complex with two unpaired electrons located on the Mg and ATP subsystems (Figure 3, left), followed by the production of two highly active radicals – •OH and $\bullet AMP^{-}$, which successively attack the inert AMP/(AMP chain) (Figure 3, right) by converting it, first, into an active radical and, second, by adding to this newly produced radical the $\bullet AMP^{-}$ radical via a spin-sensitive radical-radical interaction.

ii) the radical mechanism of nucleotide polymerization occurs only through attacking the •OH and $\bullet AMP^{-}$ radicals the HO-$C_{3'}$ group of deoxyribose/ribose (DNA/RNA) and not through the HO-$C_{2'}$ group of ribose (RNA), Figure 3, leaving the latter exposed only to the ionic polymerization mechanism.

The results come from the CPMD simulations[24-26] at 310 K.

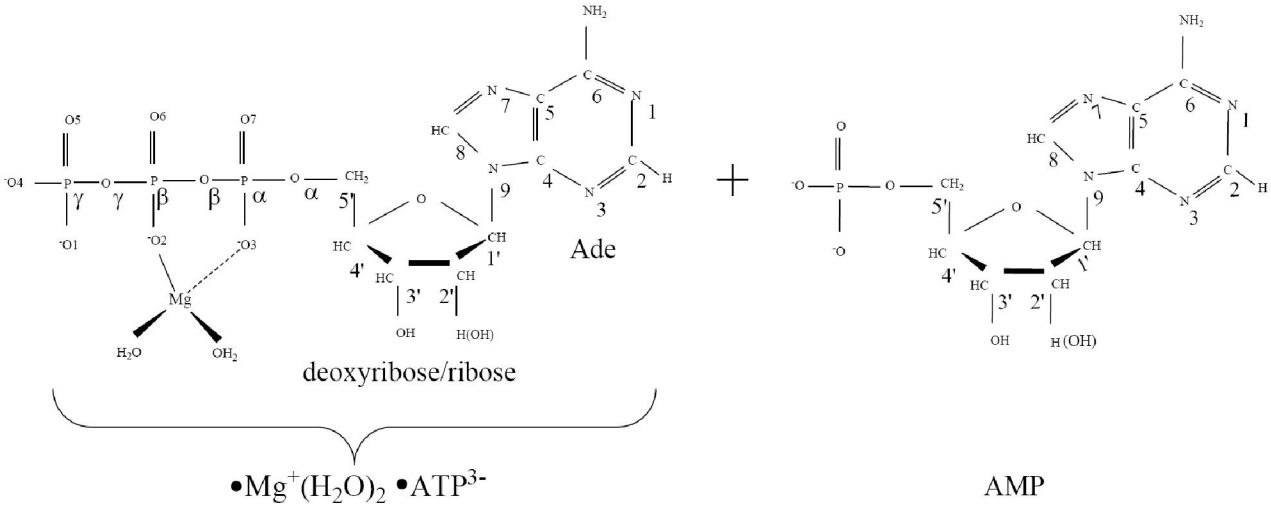

Figure 3 : Structural formulae of the [•Mg^{+}(H$_2$O)$_2$-•ATP^{3-}]^{SS} complex (left) and the AMP (right).

MODELING AND COMPUTATIONAL DETAILS

The initial geometry of the high-energy [•Mg^{+}(H$_2$O)$_2$-•ATP^{3-}]^{SS} complex (see section 1), Figure 3 (left), was obtained previously with the DFT:B3LYP, 6-311G** basis set, computations[18,19]. In this complex the Mg atom chelates the O2 oxygen atom (r[Mg-O2] = 1.98 Å) and the O3 oxygen atom (r[Mg-O3] = 2.67 Å). It should be put upfront that this way of chelation differs from that known in a stable complex [Mg^{2+}(H$_2$O)$_4$-ATP^{4-}] where the Mg binds with the O1 and O2 oxygen atoms. This uncommon chelation results from the interaction between the Mg^{2+}(H$_2$O)$_4$ complex in the lowest T state (that is a very important thing!) and the ATP^{4-}, for details see[18,19]. The difference in the total energy between the {[•Mg^{+}(H$_2$O)$_2$-•ATP^{3-}]^{SS} + 2H$_2$O + water solution} and the [Mg^{2+}(H$_2$O)$_4$-ATΦ^{4-} + water solution] is 20 kcal/mol. The initial geometry of AMP was obtained from the DFT:B3LYP, 6-311G** basis set and fits perfectly into the reported one[21].

In a cell, the polynucleotide synthesis to occur the ATP and AMP should be distanced in a range ~ 8 ÷ 4 Å[6]. This is achieved by a combined action of a holoenzyme, which activates ATP and pushes it forward to the AMP, and a template that locates the AMP (or the growing polynucleotide chain) in a fixed volume to guarantee the attack of ATP products on the AMP ribose hydroxyls[4-6]. In computations the proximity between the ATP and AMP and the AMP location is reached by a volume fixation, in which the both molecules are trapped and not allowed to escape. At the same time they are allowed to approach each other, change their configuration, and interact. Figure 4 displays the way the ATP and AMP face each other in a volume (periodic box) 16.0×9.0×18.0 Å^3. The displayed arrangement, according to the previous CPMD computations[21], is thermodynamically the most favorable among all the possible configurations. Region *ii* spans over the diphosphate part of the ATP (it leaves the ribose of the AMP sideways; the angle P$_\gamma$-P$_\alpha$(ATP)-

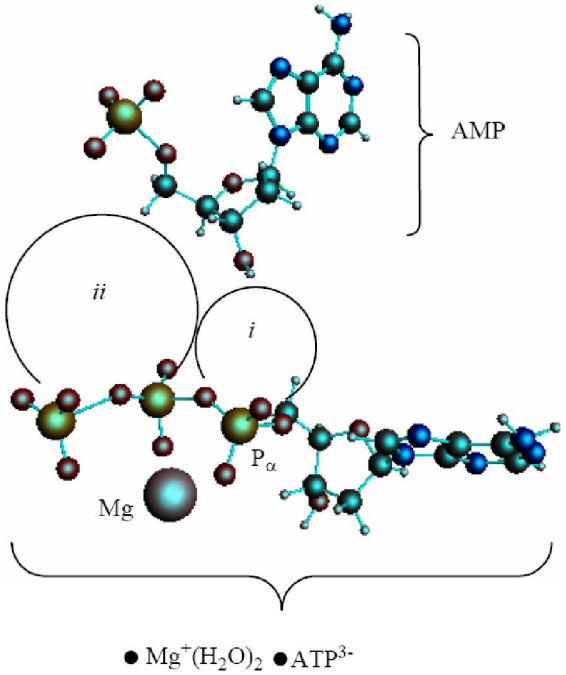

Figure 4 : The energetically favorable arrangement of the [•Mg^{+}(H$_2$O)$_2$-•ATP^{3-}]^{SS} complex and AMP. The *ii* and *i* regions indicate the P$_\gamma$O$_4$-P$_\beta$O$_3$ diphosphate and the P$_\alpha$O$_3$ monophosphate groups, respectively.

Regular Paper

O(ribose AMP) is 67^0), and region *i* – the monophosphate part (the P_α(ATP)-O(ribose AMP) distance is 5.75 Å).

One hundred and thirty two water molecules (the size of the above named box) create a water subvolume in which the Mg-ATP complex together with the Zundel cation, $H_5O_2^+$, are placed. The Zundel cation, located at the interface of *i* and *ii* regions, is introduced into the subvolume to give a chance for the •O$^-$ radical, see below, to interact with the proton and to imitate the acidic properties of living cell media. The distances between the water molecules in the periodic box, including the Zundel cation, are in the range 2.3 ÷ 2.5 Å. Such a created system ([•$Mg^+(H_2O)_2$-•ATP^{3-}]^{SS} + AMP + $H_5O_2^+$ + 132 water molecules) is then slowly heated from 0 to 310 K, for details see our previous works[18,19]. Over the heating the ([•$Mg^+(H_2O)_2$-•ATP^{3-}]^{SS} complex is forced to conserve its initial geometry to prevent its premature decomposition, Figure 3, 4.

The spin effects in the nucleotide polymerization initially assumed, the standard energy functional requires its enlargement by adding two specific terms: the *HFC* term and the *RP* term[25-28]. The inclusion of the *HFC* term is highly considerable, specifically for the phosphorus atoms, which active spin nuclei show a 100% natural abundance[29] and strongly affect the behavior of unpaired electrons in the $PO(OR)_2$ and PO_3^- radical fragments[30]. The same is valid for the active nuclear spins of hydrogen atoms (natural abundance of ^{1}H atoms with the active nuclear spin is 99.985%[24]) in water molecules and the ribose hydroxyls. In our computations the *HFC* for the named atoms includes the both isotropic and anisotropic terms; their analytical expressions might be found elsewhere[25-27]. The *RP* term includes the spin-spin electron coupling terms[27,28,31-34] arising from the interaction between the •AMP$^-$, •OH and hydrogens of water molecules and ribose hydroxyls. The interaction occurs through the exchange (2) and the dipole-dipole (3) terms:

$$\mu_B J(R)(1/2+2\sum \vec{S_i}\vec{S_j}) \quad (2)$$

$$\mu_B D(R)[\sum \vec{S_i}\vec{S_j} - 3\sum (\vec{S_i}\vec{n})(\vec{S_j}\vec{n})] \quad (3)$$

where μ_B is Bohr's magneton, $\vec{S_i}$ and $\vec{S_j}$ are the unpaired electron spins *i* and *j* located on the appropriate atom (group of atoms); the summation spans over all possible *i* and *j*. The functions $J(R)$ and $D(R)$ describe the strength of the exchange and dipolar couplings and are assumed, as is often done, to take the simple functional forms

$$J(R)=J_0 e^{-\beta R} \quad (4)$$

$$D(R)=\mu_B / R^3 \quad (5)$$

In Eqs. (2)–(5) R is the edge-to-edge distance between the radicals, J_0 is the exchange coupling constant, n is the unit vector in the direction of R and β is the range parameter. One can see that the exchange and dipolar coupling parameters decrease rapidly with the distance between the radicals and can be neglected if the distance between the radicals is sufficiently large. The characteristic distances can be estimated from the mutual geometry of ATP and AMP, see above. Their initial values are as follows: $R(P_\alpha O_3$(ATP)–HO-$C_{3'}$(AMP)) = 5.75 Å, $R(P_\alpha O_3$(ATP)–HO-$C_{2'}$(AMP)) = 9.02 Å, and $R(P_\alpha O_3$(ATP)–•OH) = 10.8 Å (these values allow the •OH to diffuse through the water volume at large distances). Note that varying $R(P_\alpha O_3$(ATP)–HO-$C_{3'}$(AMP)), see above, automatically affects the other distances. The values for J_0 and β, typical for radical pairs in solution, are taken from the previous works[34,35] and correspond to $J_0 = 7 \times 10^9$ G and $\beta = 2.15$ Å^{-1}. The estimated values for the dipolar coupling parameters are $D(R(P_\alpha O_3$(ATP)–•OH) = 75G, $D(R(PO_3$(ATP)–HO-$C_{3'}$(AMP)) = 20G, and $D(R(P_\alpha O_3$(ATP)–HO-$C_{2'}$(AMP)) = 5G. Despite the fact that these values are much smaller than those for $J(R)$ their contribution however is still remarkable at small distances.

The CPMD simulations are performed using the CPMD code, version 3.9.1[36]. The gradient-corrected BLYP functional[36] is used with a plane-wave basis (cut-off: 70.0 Ry) and norm-conserving pseudopotentials of Troullier-Martins type[30-32]. The temperature of the simulation is set to 310 K. For the solvated system like ours the thermostatting is accomplished by rescaling the kinetic energy of the nuclei whenever the temperature is deviated more than a specific tolerance[35] (± 10 K) from the desired 310 K temperature. The CPMD runs, totaling 120 (this is done to accumulate representative statistics), span over the time interval 10^{-6} s and are performed on the ultra-dense massively parallel computer cluster operating under the IBM BlueGene/L[37] (University of Minnesota, Rochester). Additionally, the implemented CPMD method includes the nonadiabatic

evolution, the so-called surface hopping method[38], when the potential energy surfaces (PESs) are as close as ≤ 2.5 kcal/mol.

SPIN-DEPENDENT DNA/RNA POLYMERIZATION: SIMILARITIES AND DISTINCTIONS

As soon as the geometry of the $[\bullet Mg^{+}(H_2O)_2\text{-}\bullet ATP^{3-}]^{SS}$ complex is unfixed (the system is thermostatted at 310 K), the complex begins to decompose. The decomposition in the water environment spans over 5.4 ps and practically does not affect the geometry of AMP. Except for the two PO_3^- molecules of ionic nature the rest products of the $[\bullet Mg^{+}(H_2O)_2\text{-}\bullet ATP^{3-}]^{SS}$ cleavage are highly reactive. The charge on the Mg atom in the $\{O_3P_\beta\text{-}Mg(H_2O)_2\}$ fragment (Figure 5a), one of the decomposition products, reaction (1), is not exactly 1.0 but 0.49, TABLE 1. The $\{O_3P_\beta\text{-}Mg(H_2O)_2\}$ fragment is not stable: the Mg undergoes a reduction (the charge on the Mg atom progressively increases from +0.49 to +1.48, TABLE 1) accompanied by transferring the electron density onto the initially uncharged atomic oxygen O, for details see[18], thus producing the $\bullet O^-$ radical. The electron transfer is coupled with the proton transfer from the Zundel cation onto the $\bullet O^-$, Figure 5a,b (structure 1,2, TABLE 1). The coupled electron/proton transfer (CEPT) however is not instantaneous. At the very beginning of the process the Mg atom is slightly charged, q(Mg) = 0.49, that makes it lose its primarily bound ligands: the two H_2O molecules and the PO_3^- fragment (the Coulomb attraction between the positively charged Mg and the negatively charged oxygens is decreased). This, specifically, is reflected on lengthening the bond distances between the Mg atom and the OH_2 molecules, 2.14 and 2.18 Å, and the $^-O_3P_\beta$ fragment, 2.64 Å, TABLE 1. The electron transfer onto the O increases the charge on the Mg atom up to 1.48 that in turn assists accumulation of a water coat around the Mg (the Coulomb attraction between the Mg and oxygens increases, but not with the PO_3^- which to that moment is 3.77 Å distanced from the Mg). This is, specifically, observed in approaching the water molecules to the Mg (structure-2), Figure 5b, TABLE 1, and adding new water molecules from the water reservoir (not shown), see section IV, that favors restoring the most stable in water $Mg(H_2O)_6$ configuration[16]. The restoring of the $Mg(H_2O)_6$ is not directly coupled with the electron pumping onto the O and the proton transfer on it from the Zundel cation, Figure 5a,b. The processes are separated in time: the first acquires milliseconds, while the latter proceeds in a picosecond – nanosecond interval[18,19]. Figure 5a shows that initially the spin density (green) is redistributed between the Mg and O atoms with the Mg slightly bound to the water molecules and the PO_3^-. As the electron density is pumped on the O, the spin density shows its localization right on the said atom, Figure 3b, which becomes a radical $\bullet O^-$. The formation of the radical assists the capture of the proton initially belonged to the Zundel cation, Figure 5a,b. The fast PCET process avoids a high-energy intermediate and undergoes a concerted mechanism[39-42] that is still valid for our system. The barrier of 1.25 kcal/mol arises from the elongation of the bond length between the H^+ and H_2O in the Zundel cation (0.96 Å → 1.07

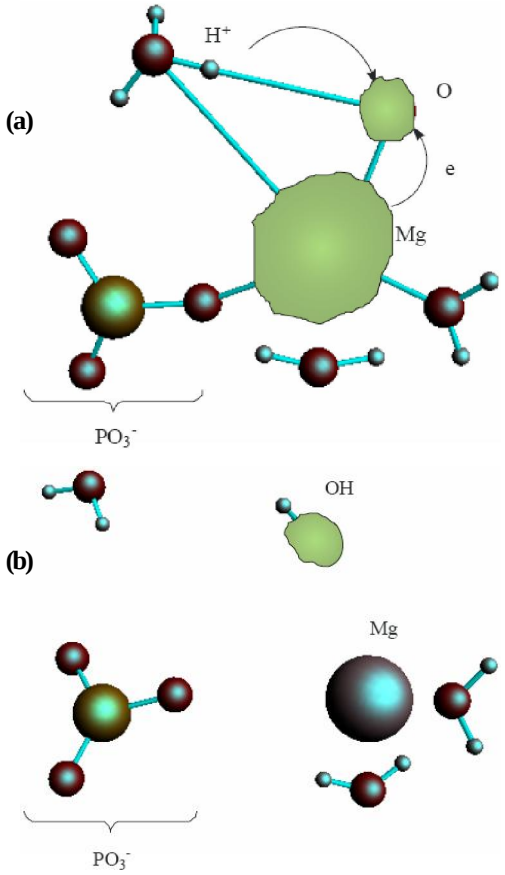

Figure 5 : The proton coupled electron transfer in the $Mg(H_2O)_2$–Zundel cation ($H_5O_2^+$, only its H_3O^+ fragment is shown)–O^- (oxygen radical) fragment: a) the initial stage of the process b) the final stage of the process, when the proton from the Zundel cation is transferred onto the oxygen radical. In green is shown a spin density distribution.

Regular Paper

Å). The elongation is accompanied by the electron pumping on the O. All in all, the decrease in total energy on arising •OH equals to -5.87 kcal/mol. This, specifically, is achieved through separating the Mg and PO_3^-, TABLE 1. Without separation the total energy decrease is much smaller, - 0.65 (a pure CPET process), and still close to that of the thermal motion, which could make the process reversible. The separation between the Mg and the PO_3^- spans over 45 ps with regard to the solvent-reactant reorganization, which in our case includes the approach of two water molecules to the Mg atom (Figure 5b), TABLE 1, and the approach of two PO_3^- fragments with further production of PP_i (milliseconds)[4-6,18], partly it is seen in Figure 6a,b.

TABLE 1 : Interatomic distances (Å) and the charge (Löwdin) on the Mg atom in the structures 1 and 2, Figure 5a, b

Distance (Å)/ charge (q)	structure-1, Figure 5a	structure-2, Figure 5b
Mg-O	2.64	3.45
H_2O-H…O	3.13	4.50
Mg-OH_2(1)	2.14	2.18
Mg-OH_2(2)	2.06	2.04
Mg-OPO_2	2.64	3.77
q(Mg)	0.49	1.48

Though the separation between the Mg and PO_3^- is a crucial process in decreasing the total energy of the system it cannot guarantee recombination between the •AMP^- (reaction (1)) and •OH. The recombination is thermodynamically favorable: the energy gain via the recombination equals to -7.87 kcal/mol. This value is lower than the previously named one -5.87 kcal/mol, see above. If the recombination occurs, instead of two highly reactive radicals we have an inert anion – a traditional AMP. The mechanism that prevents recombination lies in the spin symmetry of the •AMP^-–•OH radical pair where the spins on the •AMP^- and •OH get the identical orientation, the T_- energy state[43,44]. When in 'cage', such a radical pair with the identically oriented electron spins prefers being separated rather than being recombined[45-47]. The reason for keeping the spins parallel on the both radicals is in the highly large *HF* constant α, produced by the •AMP^- radical[30]. According to our computations (CPMD, section IV), the value of α reaches 0.078 T. The strong magnetic coupling between the ^{31}P atom and the unpaired electron on the AMP^- aligns the spin of •OH (the α in the •OH-($5H_2O$) complex at 310 K is 0.036 T – a result of the •OH magnetic field enhancement by surrounding water molecules[47]) in the identical direction to that on the •AMP^-, and the environment cannot destroy the effect in the distance range 4.75 ÷ 1.50 Å between the •AMP^- and OH. The finding is crucial for the radical polymerization to occur, see below. Moreover, the unpaired spins in the T_- state experience repulsion while the oppositely oriented spins, T_0 state, show attraction[45,46].

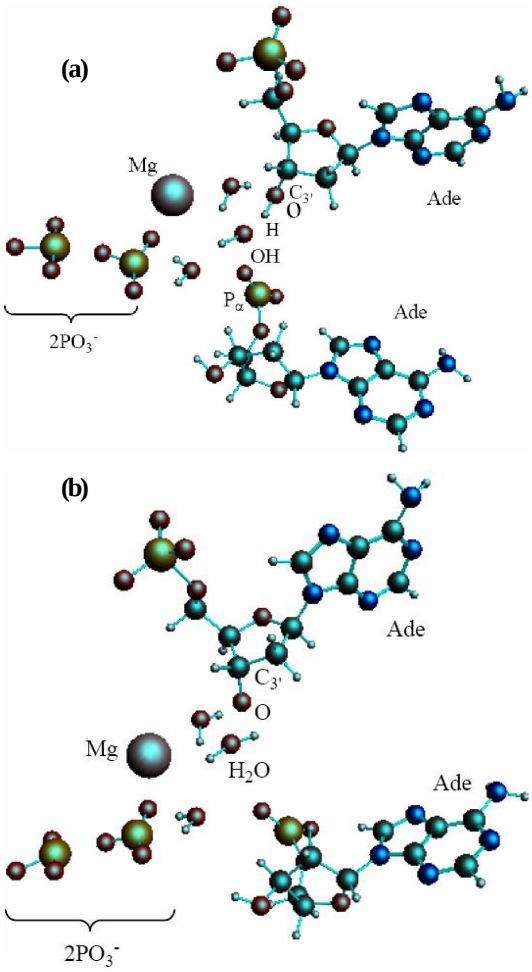

Figure 6 : The arrangement of the [•$Mg^+(H_2O)_2$-•ATP^{3-}] cleavage products and the AMP. a) the •OH radical comes close to the H-O-$C_{3'}$ group of the ribose b) the same picture when the hydrogen atom is detached from the H-O-$C_{3'}$ group and transferred onto the •OH radical with the production of water.

After the •OH production, it begins to move away from the •AMP^- toward the HO-$C_{2'}$ group of the AMP deoxyribose/ribose (the initial distance between the produced •OH and •AMP^- is 1.85 Å). The diffusion is accompanied by multistep structural rearrangements of the OH radical in the 'water tube' (2.65 Å in length) of 11 (the first and second shells) water molecules. These rearrangements are the result of hydrogen bond form-

ing/breaking between the •OH and water molecules; the O-H bond length in the radical varies in the interval – r_{max}(O-H) = 1.12 Å, r_{min}(O-H) = 0.96 Å – that coincides with the previously observed data[41]. When the •OH is as close to the HO-$C_{2'}$ as 1.54 Å, the H-O bond in the HO-$C_{2'}$ displays a progressive lengthening. This is partly due to the electron density pumping on the H from the OH and the AMP. The •OH diffusion and the H-O lengthening are accompanied by a solvent-reactant reorganization (the reorganization spans over 85 ps after the production of •OH), which finally yields the structure shown in Figure 4a. In this structure the P_{α}-O-$C_{2'}$ bond is 4.51 Å, the HO•–H-O-$C_{2'}$ bond is 1.23 Å, and the H-O bond in the HO-$C_{2'}$ is 1.07 Å. The Mg atom is separated from the PO_3^- by 4.03 Å and the two PO_3^- fragments are quite close to each other (the P_{β}-P_{γ} bond is 2.37 Å). The further approach by 0.1 Å between the •OH and the AMP results in an instantaneous hopping of the hydrogen atom on the •OH, Figure 4b. One can see that the hopping does not practically affect the solvent-reactants geometry. The hydrogen atom detachment from the deoxyribose/ribose ring is energetically favorable, -2.37 kcal/mol. This is in agreement with other theoretical findings upon the action of •OH on DNA-base fragments[42].

The hydrogen atom detachment from the deoxyribose/ribose converts the AMP into a radical, •O-$C_{3'}$(AMP), denoted hereinafter as •AMP, Figure 4b, according to reaction 2.

$$\bullet OH + HO\text{-}C_{3'}(AMP) \rightarrow H_2O + \bullet AMP \qquad (6)$$

The spin orientation on the both radicals, •AMP^- and •AMP, is opposite, the T_0 state,[39] that according to the radical pair theory serves the basis for their mutual approach via a diffusion mechanism[39,40]. The diffusion is the most time-consuming part of the process: it spans over 2.7 ns. The final stage of the process proceeds as following. The •AMP^- attacks by its phosphorus atom P_{α} (q = 1.15) the oxygen atom of the •O-$C_{3'}$(AMP) fragment (q(O) = -0.87) thus forming the adenine (Ade) dinucleotide $\{AMP\text{-}AMP\}^{3-}$ of non-radical nature, Figure 7, 8. The T_2 state (the T_2 and S_2 states stand for the dinucleotide, Figure 8), in which the spins are still unpaired and located at the Ade bases, is higher in energy than the S_2 state by 7.13 kcal/mol, a value comparable to hydrogen bonding between the complementary nucleotides in DNA. The presence of unpaired spins on the Ade bases in the T state is closely linked to complementary recognition of nucleotides upon formation of DNA duplex and spin nature of the genetic code[43]. In Figure 7 one can see that the Ade bases are essentially parallel. The further stabilization of the dimer (the process show a little decrease in the total energy of the dimer over the time) assumes the solvent reorganization around it and formation of hydrogen bonds favoring stacking between the Ade bases. This is the time-consuming process that spans in general over the millicecond interval (this interval is beyond the accepted computational interval and might be thought as an imaginary asymptotic limit). The same is valid for the PP_i formation of the two PO_3^- fragments and complete magnesium oxidation accompanied by producing the stable $Mg^{2+}(H_2O)_6$ complex that is able to act anew as a catalyst in ATP cleavage[19].

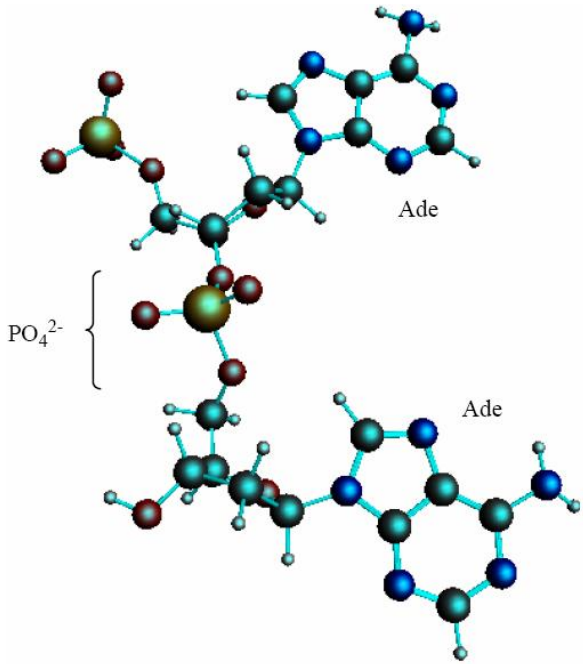

Figure 7 : Formation of the adenine dinucleotide in the singlet (S_2) state, for details see text and Figure 6.

The replacement of deoxyribose by ribose (DNA nucleotide → RNA nucleotide), which besides the HO-$C_{3'}$ group possesses the additional HO-$C_{2'}$ group, basically opens the way for attacking the latter by the •OH radical. But this does not occur, and the background for this is not only in a steric hindrance. The point is that the removing of the •OH from the •AMP^- results in the loss of the initial strong spin-spin coupling between the two radicals as the distance between them increases (eqs. (4), (5)). The weakening of the spin-spin coupling allows the hydrogen spins of surrounding water

Regular Paper

molecules to invert the initial •OH radical spin direction. With such an inverted spin, the •OH tends through the reverse diffusion to recombine with the •AMP$^-$ to form a non-radical AMP molecule that blocks the radical polymerization mechanism. The said shows the difference in operating the HO-$C_{3'}$ and HO-$C_{2'}$ groups: the former is a lucky target for the radical polymerization while the latter is still unlucky. Supposedly, the nature has made its choice in favor of the HO-$C_{3'}$ group not occasionally. The idea finds its explanation in Figure 8. The S state of AMP, S_1, lies lower than the T state, T_1, ΔE^{S-T} = - 4.3 kcal/mol. Note that this value drastically differs from that observed earlier in quantum chemistry computations for pure bases (E^{S-T} equals to several eV that corresponds to the vertical excitation with no rearrangement in geometry of nucleotides) stripped off their phosphate groups and the deoxyribose/ribose ring[46,47]. The explanation is quite simple: the attached phosphate groups and the solvent hugely affect the monophosphate nucleotide geometry making the S and T states come closer[19]. The S_1 and T_1 states have a crossing, ΔE = 6.28 kcal/mol, that is exposed to an additional crossing from the T curve corresponding to the produced •AMP$^-$-•OH radical pair. Because of the instability nature of the latter product the T curve goes straight down, and after passing the crossing point displays the formation of a dinucleotide of the T_2 (unstable state) or S_2 symmetry (stable state). The combined T-T_1-S_1 crossing occurs only when the polymerization proceeds through the HO-$C_{3'}$ group. When the HO-$C_{2'}$ group, instead of the T curve we have the T^* curve that goes above the T, crosses the S_1 and T_1 curves and does not lead to a dimer production, Figure 8. The appearance of the T-T_1-S_1 crossing (CP point in Figure 8) is highly essential because at this very crossing point the redistribution of spins occurs as shown in Figure 9. Initially, at the T_1-S_1 crossing the both triplet and singlet states are degenerated. The attack on this state from the •OH leads to electron detachment with the production of the •AMP radical that experiences an immediate attack by the •AMP$^-$ radical spin, Figure 9 (right).

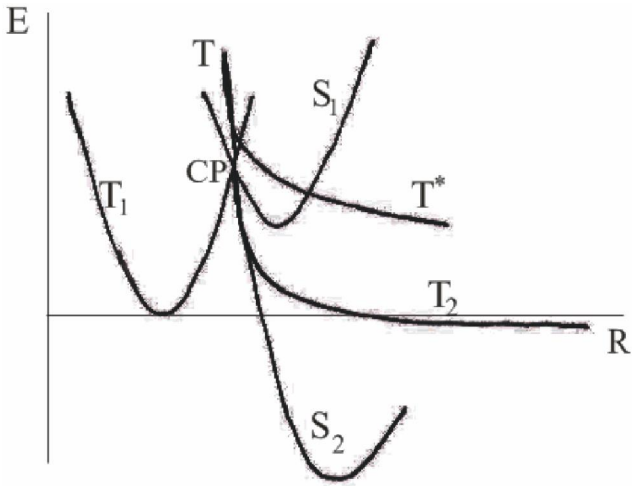

Figure 8 : The potential energy surface (PES) projections onto the energy (E) – atomic configuration (R) plane, for details see text. The blurring around the solid lines indicates 'on the fly' deviations in the CPMD computation runs. CP stands for a S_1-T_1-T crossing point.

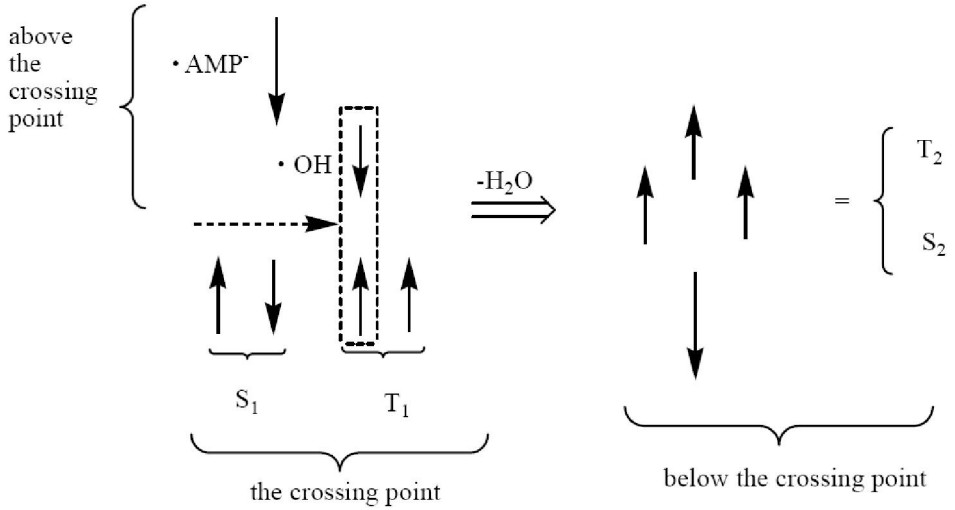

Figure 9 : Spin orientation (spins like in classical physics are shown with arrows) in the vicinity of the crossing point (CP). Above the CP we have the T state coming from the identical orientation of spins located on the •OH and •AMP$^-$. At the CP we have the S_1 and T_1 states, for details see text and Figure 6. The spins in the box form the singlet state (indicated with the rightward-pointing dashed arrow) corresponding to production of the H_2O molecule. When the latter is removed (the •OH had interacted with the AMP) we have four spins corresponding to the S_2 and T_2 states that lie below the CP (Figure 6).

This produces the S_2 and T_2 reaction paths, which initially go together and then break down into the stable and unstable states, Figure 8. The T^* curve reveals no T^*-T_1-S_1 crossing point at which an adequate interspin shuffling might occur.

CONCLUDING REMARKS

The outlined radical mechanism of nucleotide polymerization, which is realized through the HO-$C_{3'}$ bond but not through the HO-$C_{2'}$ bond, is seen more natural than the alternative ionic/hydrolytic mechanism.

First

It proceeds much faster than the ionic mechanism and includes highly reactive species, which production in a living cell under certain conditions is a common thing.

Second

It is reasonable to assume that the nature has developed this radical mechanism over a huge period of evolution with a great thought: the mechanism is highly specific and sensitive to the environment and local weak electromagnetic fields, which are able to switch the course of reaction and direct its progress over one or other potential energy surfaces.

Third

The radical mechanism was not found earlier for a very simple reason: to detect this mechanism new computational methods and experimental techniques, like CIDNP method[18,19], are required. They were unavailable as early as decades ago.

Fourth

The final products in the radical and pure ionic mechanisms are absolutely identical: these products are water, a polynucleotide, and a regenerated Mg cofactor.

Fifth

The time to complete the polymerization cycle takes milliseconds. If this time is multiplied by a number of polymerizing units, the rate of assembling nucleotides per second gives a value of 50-70 that fully agrees with the experiment[4-6].

The findings of the current work have far-reaching outlooks. They allow us to consider DNA and RNA strands as a result of interaction between the fragments of radical nature. This in turn assumes including into consideration PESs of S and T origin, which permit or forbid, respectively, H-bond recognition or non-recognition between the nucleotide interstrands. Additionally, the findings open a huge area of research concerning intercalation of drugs into the DNA helix upon manipulation of their spin states.

ABBREVIATIONS

DNA - deoxyribonucleotide acid
RNA - ribonucleotide acid
NTP - nucleosidetriphosphate
NMP - nucleisidemonophosphate
A - adenine
G - guanine
C - cytosine
Thy - thymine
U - uracil
T - triplet state
S - singlet state
PES - potential energy surface
CI - conical intersection
RP - radical pair
CIDNP - chemically induced dynamic nuclear polarization
PCR - Polymerase Chain Reaction
MTs - microtubules
MD - molecular dynamics
CPMD - Car Parrinello MD
SS - spin-separated complex/state
HFC - hyperfine coupling constant

REFERENCES

[1] I.Newton; Philosophiae Naturalis Principia Mathematica, A.Koyré, I.B.Cohen, (Ed); Cambridge, MA, **(1972)**.
[2] J.D.Watson, F.H.C.Crick; A structure for deoxyribose nucleic acid. Nature, **171**, 737-738 **(1953)**.
[3] G.Paun, G.Rosenberg, A.Salomoa; DNA computing. Springer, Berlin, **(1998)**.
[4] A.Kirschning; Immobilized catalysis. Springer Verlag, Berlin-New York, **(2004)**.
[5] F.L.Harvey, A.Berk, C.A.Keiser, M.Krieger, M.P.Scott, A.Bortscher, H.Ploegh; Molecular cell biology. Freeman, W.H. Publ., NewYork, **(2008)**.

Regular Paper

[6] D.E.Metzler; The chemical reactions of living cells. Acad. Press, New York -London, **(1977)**.

[7] J.A.Cowan; Introduction to the biological chemistry of magnesium. VCH, New York, **(1995)**.

[8] C.B.Black, J.A.Cowan; Magnesium-dependent enzymes in general metabolism. The biological chemistry of magnesium, VCH, New York, **(1995)**.

[9] L.Yang, K.Arora, W.A.Weard, S.H.Wilson, T.Schlick; Critical role of magnesium ions in DNA polymerase closing and active site assembly. J.Am.Chem.Soc., **126(27)**, 8441-8453 **(2004)**.

[10] J.M.Beechero, M.R.Otto, L.B.Bloom, R.Eritja, L.J.Reta-Krantz, M.F.Goodman; Exonuclease-polymerase active site partitioning of primer-template DNA strands and equilibrium Mg^{2+} binding properties of bacteriophage T4DNA polymerase. Biochem., **37(28)**, 10144-10155 **(1998)**.

[11] A.Kornberg, T.A.Baker; DNA replication. Second Edition, Nui Sci. Books, New York, **(2005)**.

[12] C.S.Tsai; Biomacromolecules. Introduction to structure, function and informatics. John Wiley & Sons Inc., New Jersey, **(2007)**.

[13] K.B.Mullis; The polymerase chain reaction. Nobel prize lecture: 1993. World Sci. Publ., Singapore, **(1998)**.

[14] M.Lopus, M.Yenjerla, L.Wilson; Microtubule Dynamics (Advanced Review). In: L.Wilson (Ed); Wiley Encyclopedia of Chemical Biology, Wiley & Sons, New York, 153-168 **(2009)**.

[15] W.A.Engelhardt, M.N.Ljubimova; Myosine and adenosinetriphosphatase. Nature, **144(3650)**, 668-669 **(1939)**.

[16] T.M.Kachur, D.B.Pilgrim; Myosine assembly, maintenance and elongation in muscle: Role of the chaperon unc-45 in myosine thick filament dynamics. Int.J.Mol.Sci., **8(8)**, 1863-1875 **(2008)**.

[17] J.A.Cowan; Structural and catalytic chemistry of magnesium-dependent enzymes. BioMetals, **15(3)**, 225-235 **(2002)**.

[18] A.A.Tulub; Mg spin affects adenosinetriphosphate activity. PMC Phys.B., **1(6)**, 1-18 **(2008)**.

[19] A.A.Tulub; Molecular dynamics DFT-B3LYP study of guanosinetriphosphate conversion into guanosinemonophosphate upon Mg(2+) chelation of alpha and beta oxygens of the triphosphate tail. PCCP, **8(18)**, 2187-2192 **(2006)**.

[20] V.Grignard; The use of organomagnesium compounds in preparative organic chemistry. Nobel Prise Lecture, **(1912)**.

[21] A.A.Tulub; Grignard reaction as a result of tunneling of the triplet branch of the reaction through a singlet barrier. Russian J.Gen.Chem., **72(6)**, 886 **(2002)**.

[22] A.A.Tulub; Spin polymerization of DNA/RNA nucleotides. Biophysics (Russia), **56(2)**, 300 **(2010)**.

[23] A.A.Tulub; Magnesium-associated proteins in drug design. Ann. Astra Zeneca Report, Stockholm-London-New-York-Tokyo, **(2009)**.

[24] R.Car, M.Parrinello; Unified approach to molecular dynamics and density-functional theory. Phys.Rev.Lett., **55(22)**, 2471-2474 **(1985)**.

[25] A.Furmanchuk, O.Isayev, O.V.Shishkin, L.Gorb, J.Leszczynski; Hydration of nucleic acid bases: A Car-Parrinello molecular dynamics approach. PCCP, **12(14)**, 3363-3375 **(2010)**.

[26] J.R.Asher, M.Kaupp; Car-Parrinello molecular dynamics simulations and EPR property calculations in aqueous ubisemiquinone radical ion. Theor.Chem.Acc., **119(5/6)**, 477-487 **(2007)**.

[27] J.R.Asher, M.Kaupp; Hyperfine coupling terms of benzosemiquinone radical anion from the Car-Parrinello molecular dynamics. Chem.Phys., **117(8)**, 69-79 **(2007)**.

[28] J.R.Asher, N.L.Doltsinis, M.Kaupp; Extended Car-Parrinello molecular dynamics and electronic g-tensors study of benzoquinone radical. Magn.Res.Res., **43(1)**, 237-247 **(2005)**.

[29] C.F.Matta; Quantum biochemistry. Wiley-VCH Verlag, Weinheim, **(2010)**.

[30] R.Freeman; A hndbook of nuclear magnetic resonance. Longman Sci&Tech Publ. UK, **(1988)**.

[31] I.V.Koptyug, G.W.Sluggett, N.D.Ghatlia, M.S.Landis, N.J.Turro, S.Ganapathy, W.G.Bentrude; Magnetic field dependence of the ^{31}P CIDNP in the photolysis of a benzyl phosphate. Evidence for a T_{-}–S mechanism. J.Phys.Chem., **100(35)**, 14581-14583 **(2000)**.

[32] I.A.Solov'ev, K.Schulten; Magnetoreception through Cryptochrome may involve superoxide. Biophys.J., **96(12)**, 4804-4813 **(2009)**.

[33] R.Prabhakar, P.E.M.Siegban, B.F.Minaev, H.Agren; Activation of triplet dioxygen by glucose oxidase: spin-orbit coupling in the superoxide ion. J.Phys.Chem.A, **106(14)**, 3742-3750 **(2002)**.

[34] R.A.van Santen, P.Saulet; Computational methods in catalysis and materials science. Wiley-VCH Verlag, Amsterdam-Paris, **(2009)**.

[35] J.Hutter, A.Curioni; Car-Parrinello molecular dynamics on massively parallel computers. Eur.J.Chem.Phys.Phys.Chem., **1(1)**, 1-12 **(2005)**.

[36] M.Rapacioli, R.Barthel, T.Heine, G.Seifert; Car-Parrinello treatment for an approximate density-functional theory method. J.Chem.Phys., **126(12)**, 124103-115 **(2007)**.

[37] N.Allsopp, J.Follows, M.Hennecke; Unfolding the IBM & server blue gene solutions. Int.business machine corp. IBM redbooks, **(2005)**.

[38] N.L.Doltsinis, D.Marx; Non-adiabatic car-parrinello dynamics. Phys.Rev.Lett., **88(16)**, 166402-1-4 **(2002)**.

[39] S.T.Reece, D.C.Nocera; Proton-coupled electron transfer in biology. Ann.Rev.Biochem., **78(6)**, 673-699 **(2009)**.

[40] A.Kumar, M.D.Sevilla; Proton-coupled transfer in DNA on formation of radiation-produced radicals. Chem.Rev., **10(5)**, 1021-1043 **(2010)**.

[41] S.Hammes-Schiffer; Theory of proton-coupled electron transfer in energy conversion processes. Acc.Chem.Res., **42(12)**, 1881-1889 **(2009)**.

[42] J.M.Mayer, I.J.Rhile; Thermodynamics and kinetics of proton-coupled electron transfer: stepwise vs concerted pathways. Biochim et Biophys.Acta, **16(55)**, 51-58 **(2004)**.

[43] M.Goez; Photochemically induced dynamic nuclear polarization, Adv.Photochem., **23(1)**, 63-163 **(1997)**.

[44] S.Nakagura, H.Hyashi; Dynamic spin chemistry. John Wiley & Sons, New York, **(2004)**.

[45] J.A.Jones, P.J.Hore; Spin-selective reactions of radical pairs act as quantum measurements. Chem.Phys.Lett., **(2010)**.

[46] J.J.Lee, T.Oka, T.Hirada; OH radical in water studied by quantum beats on positron annihilation - the effect of water liquid structures. J.Phys.Conf.Ser., **1(1)**, 225-228 **(2010)**.

[47] Y.Wu, C.J.Mundy, M.E.Colvin, R.Car; On the mechanism of OH radical induced DNA-base damage: a comparative quantum chemical and Car-Parrinello molecular dynamics study. J.Phys.Chem. A, **108(15)**, 2922-2929 **(2004)**.